Applied Surface Science 257 (2010) 244–248

Contents lists available at ScienceDirect

Applied Surface Science

journal homepage: www.elsevier.com/locate/apsusc

Structure and elastic recovery of Cr–C:H films deposited by a reactive magnetron sputtering technique

Wei Dai[a,b], Guosong Wu[a], Aiying Wang[a,*]

[a] Division of Surface Engineering and Remanufacturing, Ningbo Institute of Materials Technology and Engineering, Chinese Academy of Sciences, Ningbo 315201, China
[b] State Key Laboratory of Solid Lubrication, Lanzhou Institute of Chemical Physics, Chinese Academy of Sciences, Lanzhou 730000, China

ARTICLE INFO

Article history:
Received 7 April 2010
Received in revised form 28 June 2010
Accepted 28 June 2010
Available online 21 July 2010

Keywords:
Cr–C:H
Carbide
Microstructure
Elastic recovery
Tribological behavior

ABSTRACT

Cr-containing hydrogenated amorphous carbon (Cr–C:H) films were deposited on silicon substrates using a DC reactive magnetron sputtering with Cr target in an Ar and C_2H_2 gas mixture. The composition, bond structure, mechanical hardness and elastic recovery of the films were characterized using energy dispersive X-ray spectroscopy, X-ray photoelectron spectroscopy, Raman spectroscopy and nano-indentation. The film tribological behavior was also studied by a ball-on-disc tribo-tester. The results showed that the films deposited at low C_2H_2 flow rate (<10 sccm) presented a feature of composite Cr–C:H structure, which consisted of hard brittle chromium carbide phases and amorphous hydrocarbon phase, and thus led to the observed low elastic recovery and poor wear resistance of the films. However, the film deposited at high C_2H_2 flow rate (40 sccm) was found to present a typical feature of polymer-like a-C:H structure containing a large amount of sp^3 C–H bonds. As a result, the film revealed a high elastic recovery, and thus exhibited an excellent wear resistance.

1. Introduction

Amorphous hydrogenated carbon (a-C:H or DLC) films have attracted extensive interests due to their unique properties including high hardness, low friction coefficient, good wear resistance as well as the optical transparency in a wide range of VIS-IR [1,2]. However, high internal stress and poor thermal stability are two major drawbacks for the widely industrial applications [3–6]. Many studies have demonstrated that the incorporation of metal elements is one of the good candidates to decrease the DLC film internal stress and improve the film thermal stability and tribological stability [6,7]. Up to now, numerous techniques have been proposed for the synthesis of metal-containing a-C:H (Me–DLC) films, including reactive magnetron sputtering (RMS) [7,8], hybrid ion beams comprising the magnetron sputtering and ion source [6,9], and cathodic arc technique [10]. Among these techniques, considering the feasibility and advantages of mass production, low temperature deposition, and convenient metal incorporation, RMS is one of the general techniques to prepare the metal-containing a-C:H films, where the incorporated metal concentration can be well controlled by varying the ratio of hydrocarbon gas and Ar. For example, Zhang et al. [11] have deposited the Al-containing a-C:H film in argon and methane gas mixture by RMS technique, and found that the films could be either the feature of sputtered metallic Al films (at low CH_4 content) or typical a-C:H films (at high CH_4 content). Accordingly, the fraction of hydrocarbon gas in the reactive mixture was of dominance factor to determine the growth behavior and properties of the films.

It is well known that the features of the obtained Me–DLC films are significantly dependent on the selected metal elements, process parameters as well as deposition instruments, and the correlations between deposition process and film properties for various used metal elements have not been fully understood yet. In this work, we would focus on the investigation of the Cr–C:H films deposited by RMS system. The composition, microstructure and mechanical properties of the Cr–C:H films were studied as a function of the acetylene flow rate in the gas mixtures. It was found that the acetylene flow rate significantly affected the film microstructure and carbon atomic bonds, and thus led to the changes in mechanical and tribological properties of the films. Specially, at high C_2H_2 flow rate, the film presented the high elastic recovery and superior wear resistance as a consequence of the formed polymeric-like amorphous carbon feature with large amount of sp^3 C–H bonds in the film.

2. Experimental details

Cr–C:H films were deposited by a DC reactive magnetron sputtering with a Cr target (99.99%) in the argon and acetylene reactive mixtures. A p-type Si (1 0 0) wafer was used as the substrate, which was cleaned ultrasonically in acetone, ethanol, deionized water and dried in air blow before putted into the vacuum chamber. Prior to deposition, all the substrates were sputter-cleaned using Ar ions for

* Corresponding author. Tel.: +86 574 86685170; fax: +86 574 86685159.
E-mail address: aywang@nimte.ac.cn (A. Wang).

0169-4332/$ – see front matter © 2010 Elsevier B.V. All rights reserved.
doi:10.1016/j.apsusc.2010.06.076

10 min with a substrate bias voltage of −100 V. The base pressure was evacuated to a vacuum of 2.7×10^{-3} Pa. During film deposition process, the work pressure was kept at about 0.4 Pa through a pressure throttle control valve. Ar gas with a flow rate of 40 sccm was introduced into the magnetron sputter gun equipped with the Cr target. C_2H_2 gas range from 0 to 40 sccm was inputted into the chamber through another gas input port. The DC power (current model) supplied to the sputtering gun was 700 W. A negative pulsed bias voltage of −100 V (350 KHz, 1.1 μs) was applied to the substrate. The deposition time was adjusted to obtain a constant film thickness of 830 ± 20 nm for all samples.

The structure and chromium concentration of the films were analyzed by field emission scanning electron microscopy (SEM) equipping with an energy dispersive X-ray spectroscopy (EDS) (Hitachi S-4800). An X-ray photoelectron spectroscopy (XPS, Japan, Axis ultradld) with Al (mono) Kα irradiation at a pass energy of 160 eV was used to characterize the chemical bonds of the deposited films. Raman spectroscopy with an incident Ar^+ beam at a wavelength of 514.5 nm was employed to clarify the carbon atomic bonds of the films. Mechanical properties were measured using the nano-indentor (MTS-G200) in a continuous stiffness measurement (CSM) mode, and the maximum indentation depth was kept at 500 nm. The characteristic hardness of the films was chosen as the value obtained at a depth where the measured value was not affected by the soft Si substrate. The tribological behavior of the films was tested on a rotary ball-on-disk tribometer at room temperature and a relative humidity of 40–50% under dry sliding conditions. The steel ball (SUJ-2, HRC 60) with a diameter at 7 mm was used as the friction counter body. During friction test, the sliding velocity was 0.1 m/s with a distance of 500 m, the applied normal load was 1 N. The wear tracks of the films and wear scars of the counter balls were studied using optics microscopy (Leica DM2500 M, Germany).

3. Results and discussion

Fig. 1 presents the cross-sectional morphology of the films deposited at different C_2H_2 flow rates. The film thickness was evaluated about 830 ± 20 nm for all samples by controlling the deposition time. Note that the films deposited at 5 and 10 sccm C_2H_2 showed a rough and less dense fracture cross-section image. However, when the flow rate of C_2H_2 increased to 40 sccm, the film became smooth and dense, as illustrated in Fig. 1(c).

The Cr concentration of the deposited films was deduced using EDS and the relative atomic composition ratio was considered as a sum of carbon and chromium, since hydrogen could not be detected by EDS. When the C_2H_2 flow rate increased from 5 to 10 sccm, the Cr concentration decreased significantly from 19.5 to 2.7 at.%. It was found that the incorporated Cr concentration could not be deduced any more from the present EDS analysis as the C_2H_2 flow rate increased to 40 sccm. This phenomenon might attribute to the "target poisoning" due to the interaction of the Cr target with the reactive gases (carbonaceous gas), which was encountered usually in Me–DLC deposition [12,13]. The surface dynamic balance between covering by carbonaceous species and cleaning by argon ions of the metallic Cr target could be a clue to understand the evolution of incorporated Cr concentration in the films. At relatively low C_2H_2 flow rate of 5 sccm, the target collision with the Ar^+ ions was strong, large amounts of metallic chromium atoms could be easily sputtered from the target surface in a high yield and transferred to the substrate, where the Cr–C:H films were formed by the chemical reactions of sputtered Cr and hydrocarbon plasmas. With increasing C_2H_2 flow rate, the target surface poisoning became serious. The metallic chromium sputtering was gradually suppressed, and at the C_2H_2 flow rate of 40 sccm, only the formed carbonaceous coverings, rather than the metallic Cr atoms, were sputtered from the target surface. As a result, the incorporated Cr concentration could not be viewed from the EDS data. In this case, it could be proposed that the film deposition was actually dominated by the carbonaceous species sputtering, which was similar to the deposition of amorphous carbon films using magnetron sputtering with graphite target.

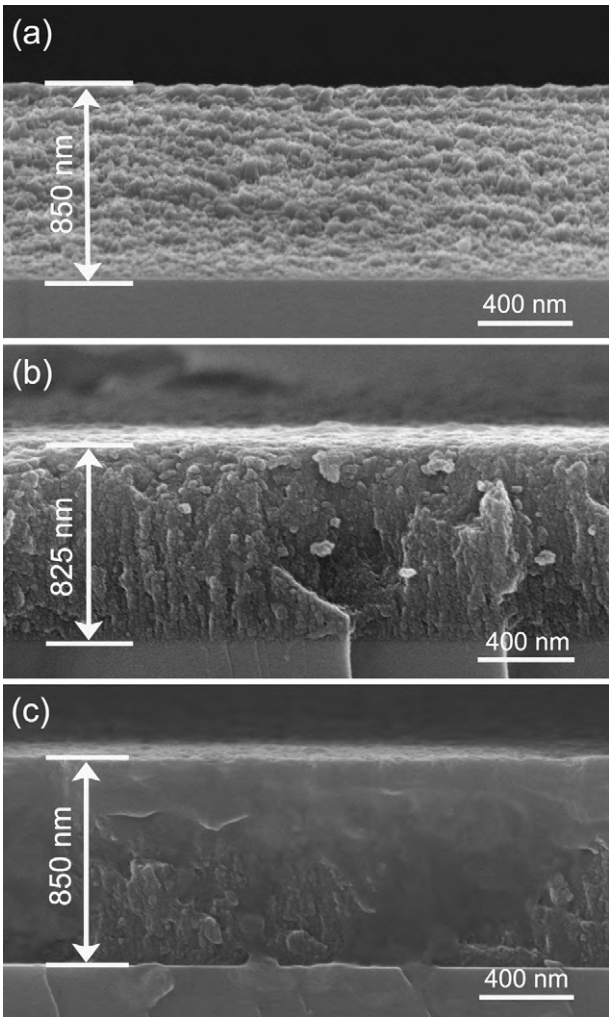

Fig. 1. SEM cross-sectional morphology of the films deposited at various C_2H_2 flow rates. (a) 5 sccm, (b) 10 sccm and (c) 40 sccm.

Further investigation of the film chemical compositions was carried out by XPS. Fig. 2 shows the representative XPS C 1s spectra of the films deposited at 5 and 40 sccm C_2H_2. Generally, the C 1s peak could be deconvoluted into three peaks around 284.5, 283.1 and 282.8 eV. The peak at 284.5 eV was correlated with the typical C–C or C–H binding energy of the a-C: H films [14], and the peaks at 282.8 and 283.1 eV were attributed to carbon in chromium carbide states of Cr_2C_3 and Cr_7C_3, respectively [15,16]. With the C_2H_2 flow rate of 5 sccm, the film revealed a major peak at a binding energy of 283 eV and a shoulder peak around 284.5 eV. This indicated that the film consisted of the dominated chromium carbide bonds and a small of hydrogenated amorphous carbon bonds. However, in the case of the film deposited at the C_2H_2 flow rate of 40 sccm, the C 1s spectrum only presented a single peak around 284.5 eV (after charging effect correction) and no carbide peak was observed, and the film exhibited the typical amorphous structure of a-C:H films.

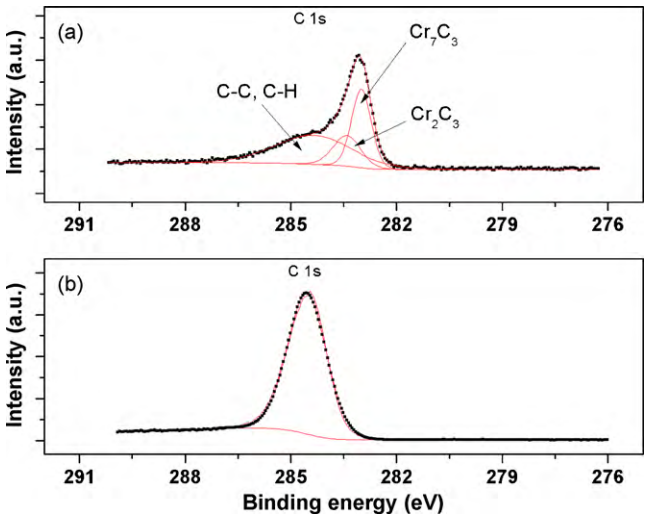

Fig. 2. Typical C 1s high resolution XPS spectra of the films deposited at C_2H_2 flow rates of (a) 5 sccm and (b) 40 sccm.

Raman spectroscopy, as a popular and non-destructive tool, is usually employed to characterize the atomic bonds of carbon films. Fig. 3 displays the Raman spectra of the Cr–C:H films deposited at various C_2H_2 flow rates. Obviously, regardless of the changes of C_2H_2 flow rate, all samples presented a broad asymmetric Raman scattering band in the range of 1000–1700 cm^{-1}, which was essentially as same as the typical carbon bond structure in a-C:H films. Raman spectroscopy can be deconvoluted into two peaks: one named of G-peak at 1580 cm^{-1} arising from E_{2g} symmetry stretching vibration mode, and another named of shoulder D-peak at around 1360 cm^{-1} caused by the zone edge of A_{1g} breathing mode [1]. According to the fitted G-peak position, the intensity ratio of D-peak to G-peak (I_D/I_G) and the full width at high maximum (FWHM)

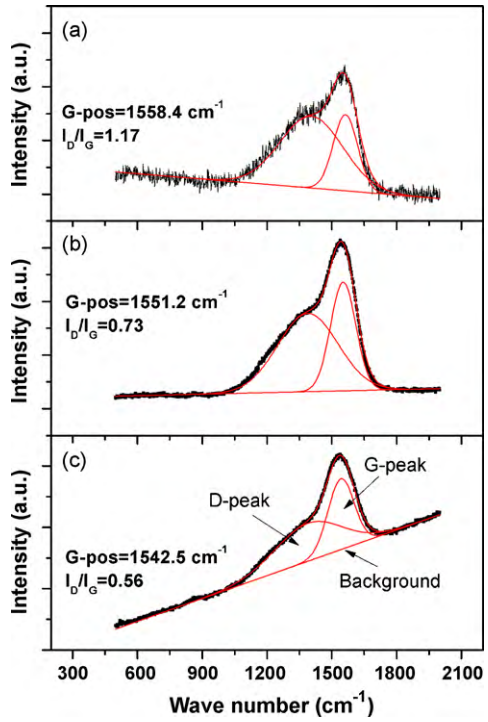

Fig. 3. Representative Raman spectra, corresponding G-peak position and I_D/I_G ratio of the films deposited at various C_2H_2 flow rates. (a) 5 sccm, (b) 10 sccm and (c) 40 sccm.

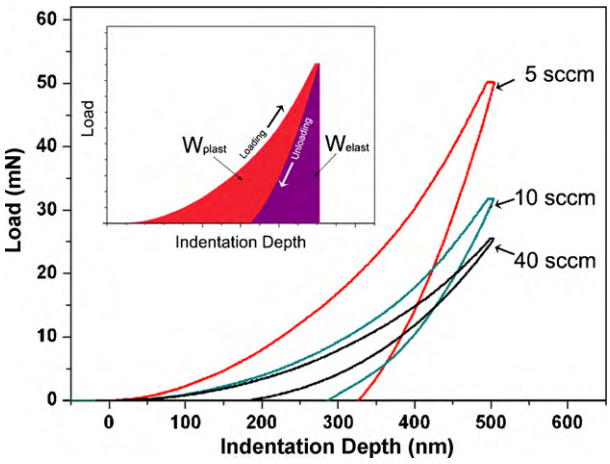

Fig. 4. Typical load-displacement curves of the films deposited at various C_2H_2 flow rates, and the insert shows the indentation work of the film.

of G-peak, the bonding structure of DLC films such as bond disorder, sp^3/sp^2 ratio, sp^2 site clustering can be derived qualitatively [17–19]. For the a-C:H films, it is empirically known that the G-peak position will shift upwards and the I_D/I_G will rise as the graphitic fraction in the film increases [1]. As Fig. 3 shows, when the C_2H_2 flow rate increased from 5 to 40 sccm, the G-peak shifted downwards sharply from 1558.4 to 1542.5 cm^{-1} and the I_D/I_G decreased from 1.17 to 0.56, implying that the sp^3 bonding fraction increased in the film, respectively. In particular, the minimum values of G-peak and I_D/I_G obtained at the C_2H_2 flow rate at 40 sccm revealed the highest sp^3 fraction in the film. Moreover, since the photoluminescence (PL) background in the visible Raman spectroscopy increased with the increase of bonded hydrogen content in a-C:H films due to the hydrogen saturation of the non-radiative recombination centers [17,18], the hydrogen variations in the films as a function of the C_2H_2 flow rate could be deduced. As can be seen in Fig. 3, the strongest PL background was observed at the C_2H_2 flow rate of 40 sccm, implying that a large amount of bonded hydrogen existed in the film. Furthermore, the increase of hydrogen content was expected to correlate with the increase of sp^3 fraction site, because the hydrogen preferably saturated the C=C sp^2 bonds and promoted the transformation from sp^2 sites to sp^3 sites [1]. As a clue, we could suppose that a polymer-like a-C:H film containing the high C–H sp^3 bonds was fabricated at high C_2H_2 flow rate (40 sccm).

Fig. 4 shows the typical nano-indentation load-displacement curves of the deposited films. The mechanical work W induced by the indentation can be divided into two parts: one part is the plastic deformation work W_p, the other one is the elastic deformation work W_e as the work of the elastic reverse deformation during the removal of the test force, as shown in the insert of Fig. 3. The ratio of the elastic deformation work W_e divided by the total work W, W_e/W, can be used as an indication of the elastic recovery to a great extent [20].

The hardness, elastic modulus and W_e/W ratio of the films deposited at various C_2H_2 flow rates are shown in Table 1. As the C_2H_2 flow rate increased, the hardness and elastic modulus

Table 1
Hardness, elastic modulus and W_e/W ratio of the films deposited at various C_2H_2 flow rates.

C_2H_2 flux (sccm)	Hardness (GPa)	Modulus (GPa)	W_e/W
5	10.6 ± 0.8	178.9 ± 7.6	0.31
10	4.4 ± 0.2	48.9 ± 1.9	0.35
40	3.6 ± 0.4	26.0 ± 1.8	0.42

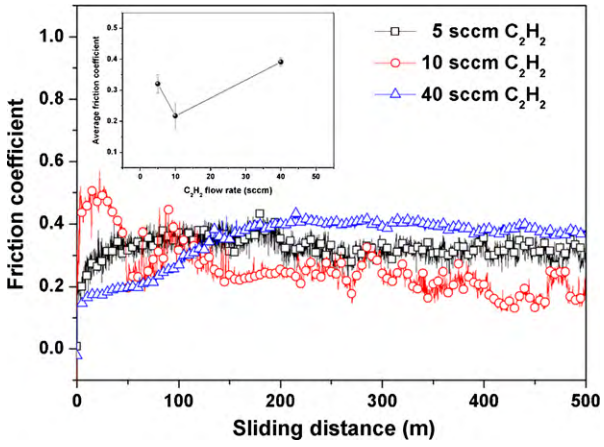

Fig. 5. Friction coefficient of the Cr–C:H films as a function of the sliding distance, and the insert shows the average coefficient of friction with different C_2H_2 flow rates.

decreased rapidly. However, the ratio of W_e/W increased significantly, implying that the elastic recovery of the films increased greatly. According to the XPS analysis, the film deposited at low C_2H_2 flow rate (5 sccm) contained a mass of hard chromium carbide phase, which would contribute to the relative high hardness. But the brittle carbide phase would also decrease the film toughness and elastic recovery [21]. Note that the film deposited at high C_2H_2 flow rate (40 sccm) showed a relative high elastic recovery ($W_e/W = 0.42$), though it exhibited a quite lower hardness. Based on the characteristics of the atomic bonding structure, it could be said that the high elastic recovery might be attributed to the existence of the formed large amount of C–H sp^3 hybridized bonds in the film, which made the film behave the typical polymer-like a-C:H feature.

Fig. 5 presents the friction coefficient evolution of the films with sliding distance. At the C_2H_2 flow rate of 5 and 40 sccm, the friction coefficients with sliding distance were relative stable beyond of the slight fluctuation in the beginning stage for each ease. While at the transition stage of C_2H_2 flow rate at 10 sccm, the friction coefficient was not stable and exhibited a significant fluctuation behavior. The average friction coefficient was calculated after about 150 m of the sliding distance, as shown in the insert figure of Fig. 5. The friction coefficient slightly decreased from about 0.3 to 0.2 when the C_2H_2 flow rate increased from 5 to 10 sccm. However, the friction coefficient increased to 0.4, as the C_2H_2 flow rate reached up to 40 sccm. The surface morphology of the wear tracks of the films and the corresponding wear scar of the contact balls after tribological tests are presented in Fig. 6. For the films deposited at 5 and 10 sccm C_2H_2, both the films and contact balls showed a deep and broad wear surfaces. While for the film deposited at 40 sccm C_2H_2, a very smooth and indistinct wear track surface emerged, and the wear scar on the sliding ball was quite smaller.

The evolution of the friction and wear behavior suggested the different wear mechanisms for the films. At low C_2H_2 flow rate (5 sccm), the film mainly consisted of the hard and brittle chromium carbide phase, which deteriorate the wear resistance of films and therefore the abrasive wear was of dominance in the wear behavior [6,21]. As the C_2H_2 flow rate increased, the content of the carbide phase decreased and amorphous carbon phase increased, which resulted in the expected decrease of friction coefficient and improvement of wear resistance. However, at high C_2H_2 flow rate (40 sccm), a larger amount of sp^3 C–H hybridized bonds were formed during the film deposition, and as a result, the film essentially performed the feature of polymeric-like carbon (PLC) with high elastic recovery and toughness. During friction process, the real contact area between the film and the counter ball would be larger due to the superior elastic deformation, which led to an increase in the friction coefficient. At the same time, the friction energy during test was partly consumed by the elastic deformation of the film and stored as elastic energy which could be released after the unloading. Accordingly, the film wear would be decreased effectively.

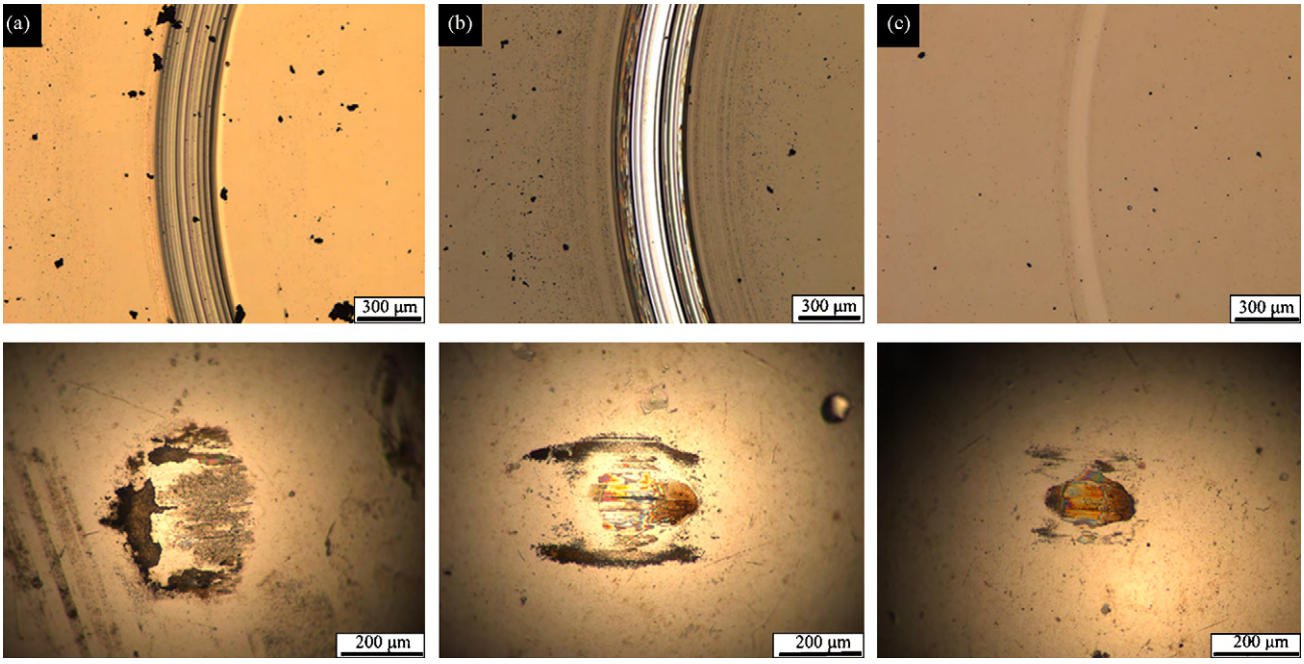

Fig. 6. Optical images of the film wear tracks (upper) and the ball wear scars (lower) at various C_2H_2 flow rates (a) 5 sccm, (b) 10 sccm and (c) 40 sccm.

4. Conclusions

The Cr–C:H films were deposited on the silicon substrates by a DC reactive magnetron sputtering with Cr target (99.99%) in the Ar and C_2H_2 gas mixture. The film deposited at low C_2H_2 flow rate of 5 sccm contained a large amount of hard and brittle chromium carbide phases, which decreased the film toughness to a great extent. As a consequence, the film behaved the high friction coefficient and wear rate. While at high C_2H_2 flow rate of 40 sccm, no chromium was observed in the film due to the significant target poisoning, which was caused by the chemical reactions between the increased hydrocarbon species and metallic chromium atoms. Accordingly, the film deposition was essentially dominated by the sputtering of the carbonaceous species covering on the Cr target, and thus resulted in the formation of the typical growth feature of polymeric-like carbon. Therefore, the film contained a larger number of sp^3 C–H hybridized bonds and performed a high elastic recovery as well as wear resistance, although it exhibited a lower hardness compared to those of the films deposited at the low C_2H_2 flow rate. The present results provided us a very good feasibility to fabricate the diamond-like carbon films with excellent elastic recovery for the certain tribological and electrical applications.

Acknowledgements

The present research was financially supported by the project of Science and Technology Department of Zhejiang Province (Grant Nos.: 2008C21055 and 2009C11SA550048) and Ningbo Municipal International Cooperation Foundation (Grant No: 2008B10046).

References

[1] J. Robertson, Mater. Sci. Eng. R 37 (2002) 129.
[2] M. Pandey, D. Bhatacharyya, D.S. Patil, K. Ramachandran, N. Venkatramani, A.K. Dua, J. Alloys Compd. 386 (2005) 296.
[3] M. Lejeune, M. Benlahsen, R. Bouzerar, Appl. Phys. Lett. 84 (2004) 344.
[4] G. Gassner, P.H. Mayrhofer, C. Mitterer, J. Kiefer, Surf. Coat. Technol. 200 (2005) 1147.
[5] G. Gassner, P.H. Mayrhofer, J. Patscheider, C. Mitterer, Thin Solid Films 515 (2007) 5411.
[6] V. Singh, J.C. Jiang, E.I. Meletis, Thin Solid Films 489 (2005) 150.
[7] C. Corbella, M. Vives, A. Pinyol, E. Bertran, C. Canal, M.C. Polo, J.L. Andújar, Surf. Coat. Technol. 177–178 (2004) 409.
[8] X.L. Bui, Y.T. Pei, J.Th.M. De Hosson, Surf. Coat. Technol. 202 (2008) 4939.
[9] A.Y. Wang, K.R. Lee, J.P. Ahn, J.H. Han, Carbon 44 (2006) 1826.
[10] Y.Y. Chang, D.Y. Wang, Surf. Coat. Technol. 200 (2006) 3170.
[11] G. Zhang, P. Yan, P. Wang, Y. Chen, J. Zhang, J. Phys. D: Appl. Phys. 40 (2007) 6748.
[12] O.A. Fouad, K. Abdul, S. Rumaiz, Ismat Shah, Thin Solid Films 517 (2009) 5689.
[13] I. Safi, Surf. Coat. Technol. 127 (2000) 203.
[14] D. Bourgoin, S. Turgeon, G.G. Ross, Thin Solid Films 357 (1999) 246.
[15] L. Ramqvist, J. Phys. Chem. Solids 30 (1969) 1835.
[16] H. Goretzki, Z. Fres, Anal. Chem. 333 (1989) 451.
[17] C. Casiraghi, A.C. Ferrari, J. Robertson, Phys. Rev. B 72 (2005) 085401.
[18] A.C. Ferrari, J. Robertson, Phys. Rev. B 61 (2000) 14095.
[19] A.C. Ferrari, J. Robertson, Phys. Rev. B 64 (2001) 075414.
[20] T. Miura, Y. Benino, R. Sato, T. Komatsu, J. Eur. Ceram. Soc. 23 (2003) 409.
[21] X. Han, F. Yan, A. Zhang, A. Zhang, P. Yan, B. Wang, W. Liu, Z. Mu, Mater. Sci. Eng. A 348 (2003) 319.